Original Article

Sexual Development

Sex Dev 2009;3:237–244
DOI: 10.1159/000252814

Received: June 2, 2009
Accepted: July 13, 2009
Published online: October 23, 2009

Functional Analysis of Novel Androgen Receptor Mutations in a Unique Cohort of Indonesian Patients with a Disorder of Sex Development

P. Elfferich[a] A.Z. Juniarto[f] H.J. Dubbink[b] M.E. van Royen[b] M. Molier[b] J. Hoogerbrugge[c] A.B. Houtsmuller[b] J. Trapman[b] A. Santosa[g] F.H. de Jong[d] S.L.S. Drop[e] S.M.H. Faradz[f] H. Brüggenwirth[a] A.O. Brinkmann[c]

Departments of [a]Clinical Genetics, [b]Pathology, [c]Reproduction and Development, [d]Internal Medicine and [e]Pediatric Endocrinology, Sophia Children's Hospital, Erasmus MC, Rotterdam, The Netherlands; [f]Division of Human Genetics, Center for Biomedical Research and [g]Department of Urology, Faculty of Medicine, Diponegoro University, Dr. Kariadi Hospital, Semarang, Indonesia

Key Words
Androgen insensitivity syndrome · Androgen receptor · FxxLF motif · Mutations · Transcriptional activation

Abstract
Mutations in the androgen receptor *(AR)* gene, rendering the AR protein partially or completely inactive, cause androgen insensitivity syndrome, which is a form of a 46,XY disorder of sex development (DSD). We present 3 novel *AR* variants found in a cohort of Indonesian DSD patients: p.I603N, p. P671S, and p.Q738R. The aim of this study was to determine the possible pathogenic nature of these newly found unclassified variants. To investigate the effect of these variants on AR function, we studied their impact on transcription activation, AR ligand-binding domain interaction with an FxxLF motif containing peptide, AR subcellular localization, and AR nuclear dynamics and DNA-binding. AR-I603N had completely lost its transcriptional activity due to disturbed DNA-binding capacity and did not show the 114-kDa hyperphosphorylated AR protein band normally detectable after hormone binding. The patient with AR-I603N displays a partial androgen insensitivity syndrome phenotype, which is explained by somatic mosaicism. A strongly reduced transcriptional activity was observed for AR-Q738R, together with diminished interaction with an FxxLF motif containing peptide. AR-P671S also showed reduced transactivation ability, but no change in DNA- or FxxLF-binding capacity and interferes with transcriptional activity for as yet unclear reasons.

Disorders of sex development (DSD) are defined as any congenital condition in which the development of chromosomal, gonadal, or anatomical sex is atypical [Hughes, 2008]. One of these disorders is caused by defects in androgen action. The androgen insensitivity syndrome (AIS) results from mutations in the X-linked androgen receptor *(AR)* gene. A great variety of mutations in the *AR* gene has been reported (www.mcgill.ca//androgendb), resulting in a wide spectrum of clinical phenotypes [Gottlieb et al., 1996].

The androgen receptor is a transcription factor that belongs to the super family of nuclear receptors and is composed of distinct domains characteristic for steroid

KARGER
Fax +41 61 306 12 34
E-Mail karger@karger.ch
www.karger.com

1661–5425/09/0035–0237$26.00/0

Accessible online at:
www.karger.com/sxd

Peter Elfferich
Department of Clinical Genetics
Erasmus Medical Centre
PO Box 2040, NL–3000 CA Rotterdam (The Netherlands)
Tel. +31 10 704 4222, Fax +31 10 704 4764, E-Mail p.elfferich@erasmusmc.nl

hormone receptors. The variable NH_2-terminal domain (NTD) is mainly involved in transcription activation [Jenster et al., 1991]. The DNA-binding domain (DBD) of the AR contains 2 zinc-clusters that specifically bind regulatory sequences in promoter/enhancer regions of androgen-regulated genes [Claessens et al., 2001]. A short flexible hinge region, containing highly positively charged amino acid residues, links the DBD to the ligand-binding domain (LBD). The AR-LBD consists of 10–12 α-helices. Upon hormone binding, helix 12 functions as a lid and fixates the hormone in the ligand-binding pocket. As a result, a hydrophobic coactivator-binding groove on the LBD-surface is created [Dubbink et al., 2004]. The coactivator-binding groove functions as an interaction surface for LxxLL- and FxxLF-like motifs containing coactivators [Dubbink et al., 2004; van de Wijngaart et al., 2006; Trapman and Dubbink, 2007] (where L is a leucine, F is a phenylalanine, and x represents any amino acid) as well as for the FxxLF motif in the AR-NTD, important in the NH_2/COOH terminal domain interaction (N/C-interaction) [He et al., 2000; Steketee et al., 2002].

Here we report 3 novel *AR* missense mutations found in a unique cohort of 101 Indonesian DSD patients. The aim of this study was to determine the possible pathogenic nature of these newly found unclassified variants. To investigate the effect of these mutations on AR function, we studied their impact on transcription activation, on AR-LBD interaction with an FxxLF motif containing peptide, on AR subcellular localization, and on AR nuclear dynamics and DNA binding. Together, these data provide a molecular explanation for the clinical presentation of these partial androgen insensitivity syndrome (PAIS) patients.

Patients, Materials, and Methods

Patients

Patient A was referred to the Dr. Kariadi Hospital, Semarang, Indonesia at the age of 12 years because of genital ambiguity. He had a male gender, and physical examination showed a bifid scrotum with palpable testes and perineal hypospadias, Quigley stage 5 [Quigley et al., 1995], and breast development, Tanner stage 3–4. His serum concentrations of LH (2.1 IU/l) and FSH (5.3 IU/l) were in the normal range for early puberty, and serum testosterone (basal 1.6 nmol/l) rose to 20.4 nmol/l 3 days after the injection of 1,500 IU of human chorionic gonadotropin (hCG), indicating an absence of disorders in testosterone biosynthesis. The serum level of anti-Müllerian hormone (AMH), which should decline under the influence of testosterone in early puberty, was relatively high (21 μg/l). He underwent surgical correction for his hypospadias and breast development. Sequence analysis revealed a mosaic missense mutation in exon 3 of the *AR* gene (c.2170 T>A) at amino acid residue 603 (according to http://www.mcgill.ca/androgendb) leading to a substitution of isoleucine with asparagine. Both parents were tested negative for this mutation.

Patient B was referred to the clinic at the age of 2.5 years because of hypospadias. He had a male gender. Testes were palpable in a bifid scrotum, and there was scrotal hypospadias, Quigley stage 2. Serum LH (<0.1 IU/l) and FSH (0.55 IU/l) were normal for his age, as was serum testosterone (<0.1 nmol/l). The level of testosterone increased to 16.9 nmol/l after administration of hCG. Serum AMH was in the normal prepubertal range (68 μg/l). Hypospadias correction was performed at the age of 3.5 years. Using sequence analysis, a missense mutation was identified in exon 4 of the *AR* gene (c.2373 C>T) leading to a substitution of proline 671 with serine. Sequence analysis of the parents revealed that the mother was a carrier of the P671S mutation.

Patient C was seen at the clinic at the age of 4.5 years because of penoscrotal hypospadias. He presented with a bifid scrotum and a micropenis (2 cm), Quigley stage 4. Serum LH (0.26 IU/l) and FSH (0.68 IU/l) were normal for his age, as was serum testosterone (0.1 nmol/l). The level of testosterone increased to 20.5 nmol/l after administration of hCG. Serum AMH was in the normal prepubertal range (158 μg/l). He underwent a hypospadias correction. Topical dihydrotestosterone (DHT) treatment with DHT cream during 3 months resulted in an increase of penis length of 1.6 cm. Using sequence analysis, a missense mutation was identified in exon 5 of the *AR* gene (c.2575 A>G) leading to a substitution of glutamine 738 with arginine. Sequence analysis of the parents' DNA revealed that the mother was a carrier of the Q738R mutation.

All these patients were of Javanese Indonesian origin, had a 46,XY karyotype and were diagnosed with PAIS.

Mutation Analysis, Site-Directed Mutagenesis, and Construction of AR Expression Vectors

Numbering of the amino acid residues is according to the National Center for Biotechnology Information (NCBI) accession number AAA51729, which refers to the AR consisting of 919 amino acid residues [Lubahn et al., 1988]. Extraction of DNA from peripheral blood cells was performed according to standard techniques. The coding exons and exon/intron boundaries of the *AR* gene were analyzed by direct sequencing on an ABI3730XL automated sequencer. All variations except known neutral variants were confirmed by a 2nd sequencing experiment on DNA of the patients.

The human wildtype *AR* cDNA expression plasmid pSG5AR, a gift from Dr. Andrew Cato, was used to generate constructs encoding the mutant *AR*s using QuickChange site-directed mutagenesis (Stratagene, La Jolla, Calif., USA). The following sense and antisense primers containing the mutated sequence (depicted in lowercase lettering) were used: for preparation of pSG5AR-I603N sense primer 5′-GTGCGCCAGCAGAAATGATTGCACTAaTGATAAATTCC-3′ and antisense primer 5′-GGAATTTATCAtTAGTGCAATCATTTCTGCTGGCGCAC-3′, for pSG5AR-P671S sense primer 5′-CTATGAATGTCAGtCCATCTTTCTGAATGTCCTGGAAGC-3′ and antisense primer 5′-GCTTCCAGGACATTCAGAAAGATGGaCTGACATTCATAG-3′, and for pSG5AR-Q738R sense primer 5′-CCAGATGGCTGTCATTCgGTACTCCTGGATG-3′ and antisense primer 5′-CATCCAGGAGTACcGAATGACAGCCATCTGG-3′. The introduction of the mutations was confirmed by sequence analysis. By

digestion with restriction enzymes and subcloning, the mutant fragments were exchanged with wildtype fragments of vector pSG5AR. For exchange of the I603N encoding fragment, digestions with *Asp*718 and *Asp*I were used. Digestions with *Asp*I and *Bam*HI were applied for the P671S and Q738R encoding fragments. Green fluorescent protein (GFP)-tagged mutant *AR* expression constructs were generated by subcloning of the mutated fragments into pEGFP-AR0 [Farla et al., 2004] by *Eco*RI and *Hin*dIII digestions. The cloning sites of all constructs were screened by direct sequencing. The Gal4-DBD-AR FxxLF expression construct has been described previously [Dubbink et al., 2004].

Measurements of Hormone Levels

Hormone levels were determined using a chemoluminescence-based immunometric method (Immulite 2000, Siemens-DPC, Los Angeles, Calif., USA) for LH and FSH, a coated tube radioimmunoassay (Coat-a-Count, Siemens-DPC) for testosterone, and an enzyme immunometric assay (DPC, Webster, Tenn., USA) for AMH.

Western Blot Analysis

For Western blot analysis COS-1 cells were seeded in 6-well plates (diameter 35 mm) at a density of 0.15×10^6 cells per well in DMEM:F12 supplemented with 100 U/ml penicillin, and 100 μg/ml streptomycin, Glutamax, 5% fetal calf serum (FCS, PerBio) treated with dextran coated charcoal. The next day the cells were transfected with either pSG5AR, pSG5AR-I603N, pSG5AR-P671S, and pSG5AR-Q738R or empty vector pSG5, respectively. For each well 0.25 μg DNA was mixed with 0.6 μl FuGENE reagent (Roche Diagnostics) in MEM medium without FCS. After 24 h 50 nM R1881 or vehicle (0.1% ethanol) was added to the wells. The next day the cells were washed with PBS. Per well 200 μl ice-cold SDS Laemmli sample buffer containing 10 mM dithiothreitol (DTT) was added and the cells were scraped with a policeman. The cell lysates were transferred to 1.5-ml Eppendorf tubes and boiled for 2 min. After a short sonication step, 7 μl of the lysate was loaded onto a 7% SDS-polyacrylamide gel. Proteins were separated and blotted onto a nitrocellulose membrane (Schleicher & Schuell, Dassel, Germany). Immunoblotting was performed using polyclonal antibody SP197 [Kuiper et al., 1993], and proteins were visualized via the ECL method (Perkin Elmer NEL101, Shelton, Conn., USA).

Luciferase (Luc) Assays

For transcription activation studies Hep3B cells were cultured in α-MEM medium (Lonza BioWhittaker) supplemented with 5% FCS, 100 U/ml penicillin, and 100 μg/ml streptomycin. One day before transfection, Hep3B cells were plated in 24-well plates at a density of 5×10^4 cells per well. After 24 h α-MEM medium supplemented with 5% FCS was replaced by α-MEM medium with 5% charcoal-treated FCS supplemented with either vehicle (0.1% ethanol) or a range of 10 pM–10 nM synthetic androgen R1881. Four hours after addition of R1881, the cells were transfected with the *AR* expression constructs using FuGENE reagent. The DNA mixture was composed of 50 ng *AR* expression construct, 100 ng ARE_2-TATA-Luc or MMTV-Luc reporter plasmid, and 1 μl FuGENE reagent per well in 25 μl α-MEM. The DNA mixture was pre-incubated for 2 h at room temperature before adding to the cells.

For interaction assays the same procedure of cell culture was used as described above. All the interaction assays were performed with or without addition of 1 nM R1881. A mixture of 50 ng *AR* expression construct, 50 ng Gal4-DBD-AR FxxLF expression construct, and 150 ng UAS4-TATA-Luc reporter plasmid was applied per well. The cells were lysed and Luc activity was measured in a Fluorescent Ascent FL (Labsystems Oy, Helsinki, Finland) 24 h after DNA transfection.

Subcellular Localization and Nuclear Mobility of GFP-Tagged AR Mutants

Two days before microscopic analysis, Hep3B cells were grown on glass cover slips in 6-well plates in α-MEM supplemented with 5% FCS, 2 mM Glutamine, 100 U/ml penicillin, and 100 μg/ml streptomycin. At least 4 h before transfection, the medium was substituted by medium containing 5% dextran charcoal-stripped FCS. Transfections were performed with 1 μg GFP-AR expression construct in FuGENE6 transfection medium (Roche). Four hours after transfection, the medium was replaced by medium with 5% dextran charcoal-stripped FCS supplemented with 1 nM R1881 when indicated.

Live cell imaging and strip-FRAP analysis were performed using a confocal laser-scanning microscope (LSM510; Carl Zeiss MicroImaging, Inc.) equipped with a Plan-Neofluar 40×/1.3 NA oil objective (Carl Zeiss MicroImaging, Inc). Enhanced green fluorescent protein (EGFP) was excited using a 488 nm laser line of an argon laser at moderate laser power to obtain images. EGFP emission was detected using a 505–530 nm bandpass emission filter.

Strip-FRAP analysis was performed as described by van Royen et al. [2009]. Briefly, fluorescence in a narrow strip (~700 nm – corresponding to 10 pixels at zoom 6) spanning the entire nucleus is bleached and the recovery of fluorescence inside this strip is monitored in time with a 21-ms interval using a low laser power. Fluorescence intensity in the strip is expressed relative to prebleach intensities and the intensity directly after bleaching.

Results

To find a possible pathogenic effect for the clinical phenotypes of the PAIS patients harboring *AR* mutations p.I603N, p.P671S, and p.Q738R, the corresponding mutant *AR* expression constructs were generated, and the effects of the amino acid substitutions on AR function were studied in vitro. We investigated hyperphosphorylation, transcription activation, AR-LBD interaction with an FxxLF peptide motif, AR subcellular localization, and nuclear mobility and DNA-binding capacity of the distinct mutants.

AR Isoform Pattern

Previous experiments have shown that in the absence of hormone, the AR protein displays a protein doublet of 110–112 kDa and an extra hyperphosphorylated 114-kDa band upon hormone binding during SDS-polyacrylamide

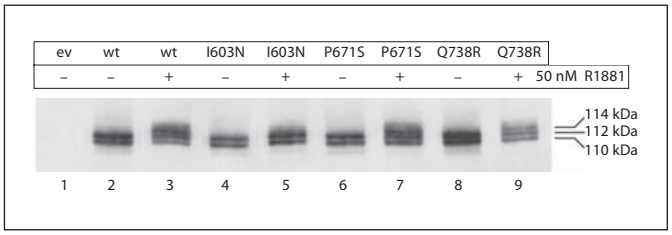

Fig. 1. Western blot analysis of PAIS-associated AR mutants. Wildtype AR (wt) and AR mutants I603N, P671S, and Q738R were expressed in COS-1 cells in the absence (–) or presence (+) of 50 nM R1881. After SDS-PAGE and immunoblotting, the AR protein was visualized by polyclonal antibody Sp197. ev = Empty vector.

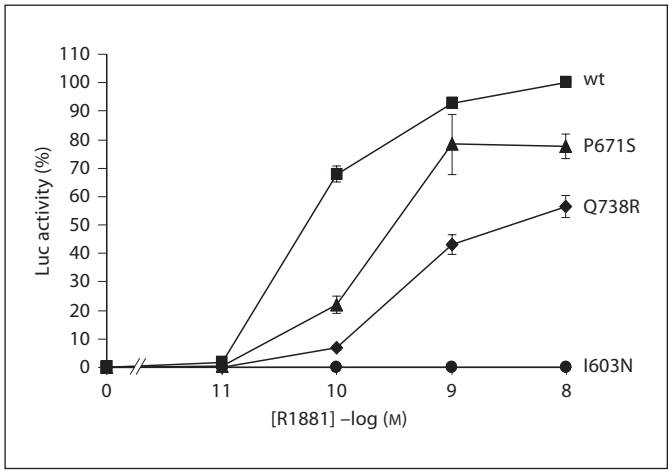

Fig. 2. Transcription activation assay in Hep3B cells. Dose-response curves of wildtype AR, AR-P671S, AR-Q738R, and AR-I603N in the presence of increasing amounts of R1881. The activity of wildtype AR at 10 nM R1881 was set at 100% and the other data points were calculated relative to that. Values represent the means ± SEM of 2 independent experiments, performed in triplicate.

gel electrophoresis (SDS-PAGE). Part of the hormone-induced phosphorylation occurs following DNA binding and during or following transcription regulation [Jenster et al., 1994]. To study the effect of the PAIS-associated *AR* mutations on phosphorylation, wildtype *AR* and *AR* mutants I603N, P671S, and Q738 were expressed in COS-1 cells by transient transfection of the distinct *AR* constructs and Western blot analysis was performed after SDS-PAGE. Figure 1 shows expression of the 110–112-kDa protein doublet by wildtype AR and all mutant ARs. However, incubation with the synthetic androgen R1881 induced expression of the hyperphosphorylated 114-kDa protein band in case of wildtype AR, AR mutants P671S and Q738R, but not of the AR mutant I603N (fig. 1, lane 5).

Transcription Activation

Next, we studied transcriptional activation by the different mutant ARs. Hep3B cells were transiently transfected with one of the *AR* expression constructs described above and an ARE_2-TATA-Luc reporter construct. Cells were incubated in the presence of increasing concentrations of R1881. The AR-I603N mutant completely lost its transactivation potential even at the highest hormone concentration tested (fig. 2). Both the Q738R and P671S mutants showed reduced maximal transactivation capacity of 56 and 78% of wildtype AR activity, respectively, in the presence of 10^{-8} M R1881. In addition, higher R1881 concentrations were required for androgen induction, as at 10^{-10} M R1881 their activities were only 10 and 32% of wildtype AR, respectively. In CHO cells and with a MMTV-Luc reporter construct, similarly reduced transcriptional activities were observed for the distinct mutants (data not shown).

Intracellular Distribution in Living Cells

To study the distribution of AR in living cells, wildtype AR, a non-DNA-binding AR mutant (AR-A573D) as a positive control, and the 3 AR mutants were N-terminally tagged with GFP. In the absence of hormone, the proteins were mainly cytoplasmic (left panels in fig. 3a–c, e, g). After addition of 1 nM R1881, the GFP-AR translocated to the nucleus (right panels in fig. 3a–c, e, g). In the nucleus AR-P671S and AR-Q738R displayed a typical punctate distribution pattern similar to wildtype AR (right panels in fig. 3a, e, g) [Farla et al., 2004; van Royen et al., 2007]. Nuclei of cells transfected with AR-I603N, however, lacked this punctate pattern and showed a more homogeneous distribution (right panel in fig. 3c), similar to the non-DNA-binding mutant AR-A573D (right panel in fig. 3b) [Farla et al., 2004].

FRAP was used to study the intranuclear mobility of the AR mutants. In concordance with their distribution pattern, AR-P671S and AR-Q738R showed a transient immobilization similar to wildtype AR (fig. 3f, h), whereas the redistribution of AR-I603N was as fast as the non-DNA-binding mutant AR-A573D (fig. 3d).

Interaction with an α-Helical FxxLF Peptide Motif

Upon hormone binding, a hydrophobic groove is formed in the AR-LBD surface. This coactivator-binding

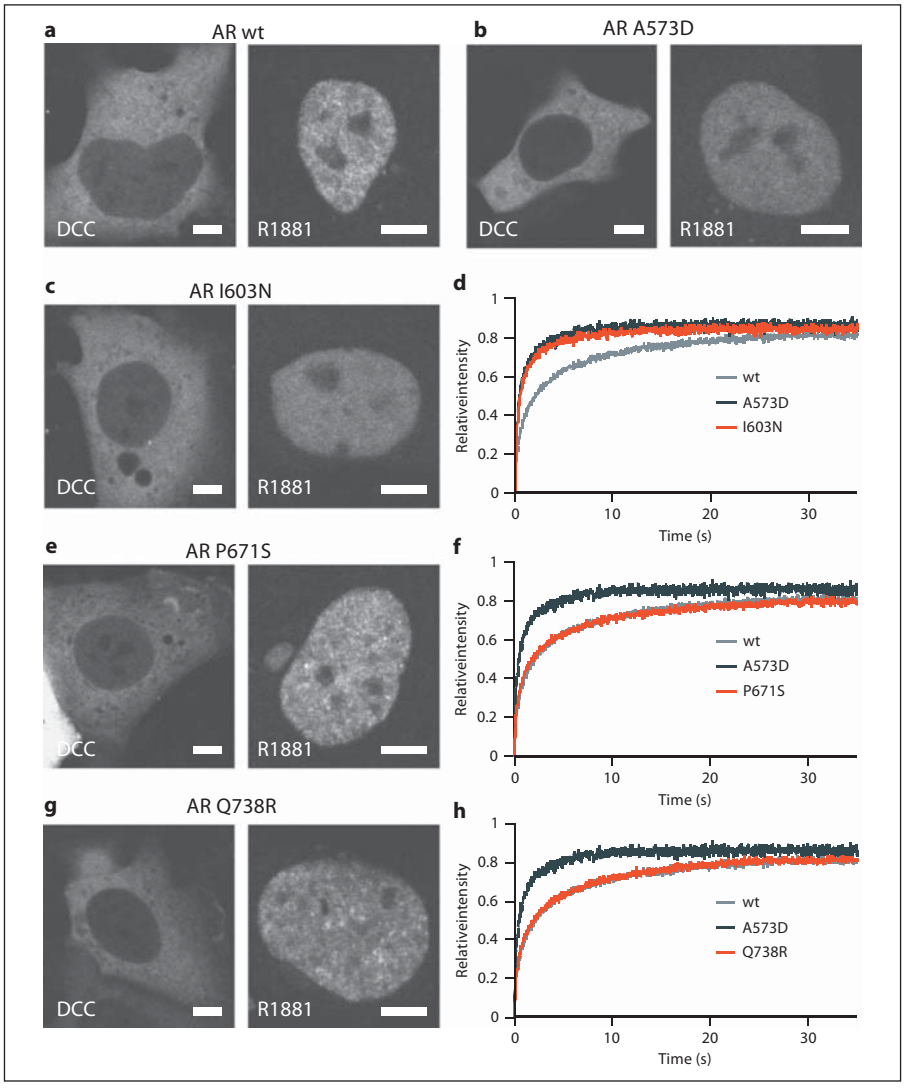

Fig. 3. High-resolution confocal images and strip-FRAP analysis of cells expressing GFP-tagged AR mutants. Confocal images of Hep3B cells expressing GFP-tagged wildtype AR (**a**) and mutant GFP constructs (**b**, **c**, **e**, **g**) in the absence (left panels) and presence (right panels) of 1 nM R1881. The nuclei in the hormone-treated cells were represented at 1.6× higher magnification as compared to the cells in the 'minus hormone' situation in order to emphasize the differences in the speckled patterns in the nuclei. Bars represent 5 μm. **d**, **f**, **h** Strip-FRAP analysis of the indicated AR mutants in the presence of 1 nM R1881 (red curves). Redistribution of wildtype AR (grey curve) and a non-DNA-binding mutant (AR-A573D) (black curve) were plotted as references. DCC = Dextran-coated charcoal.

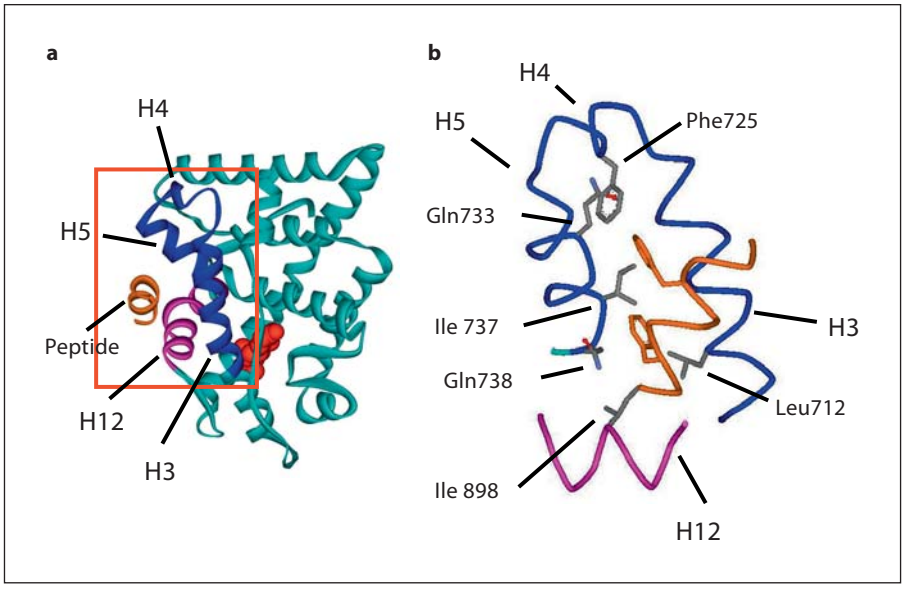

Fig. 4. Structure of the androgen receptor ligand-binding domain (LBD). **a** Ribbon representation. The ligand, positioned in the ligand-binding pocket, is indicated in red. Helices 3, 4, and 5 are shown in dark blue, helix 12 is purple. An FxxLF peptide motif interacting with the cofactor-binding groove in the LBD surface is displayed in brown. The region in the red square is enlarged and rotated in **b**. **b** Position of an FxxLF peptide (brown) in the cofactor-binding groove of the LBD. Important amino acid residues are indicated in the LBD, lining the cofactor-binding groove, in which missense mutations have a proven correlation with AIS. Colors are as shown in **a**. The figures are generated in ViewerLite 5.0 (Accelrys) using the coordinates of Protein Data Bank entry 1XOW.

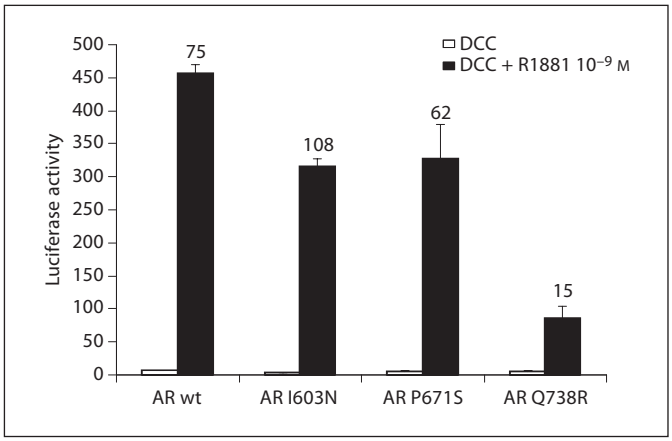

Fig. 5. Interaction assay as measured in Hep3B cells transfected with wildtype AR and AR mutant constructs. The AR FxxLF-motif peptide construct and the UAS4-TATA-Luc reporter plasmid were used in this interaction assay. Interaction was measured in the absence (open bars) and presence of 1 nM R1881 (black bars). On top of the bars, standard deviation is displayed plus the fold induction. DCC = Dextran-coated charcoal.

groove is lined by 13 amino acid residues, which reside in helices H3, H4, H5, and H12 (fig. 4), one of which is Q738 [Trapman and Dubbink, 2007]. The coactivator groove interacts with LxxLL- and FxxLF-like motifs present in AR cofactors and with the FxxLF motif in the AR-NTD. To investigate the effect of the *AR* mutations on LxxLL and FxxLF motif interaction, binding to the AR FxxLF motif was studied. For this purpose, Hep3B cells were transiently transfected with constructs expressing a Gal4-DBD-FxxLF fusion protein and full-length ARs together with an UAS4-TATA-Luc reporter construct. Experiments were done in the absence and presence of 1 nM R1881. Interaction of the AR FxxLF motif with AR-I603N and AR-P671S was strongly induced by the hormone to similar levels as shown for wildtype AR (fig. 5). However, AR FxxLF interaction with AR-Q738R was 5-fold decreased compared to wildtype AR. These data indicate that cofactor binding to the coactivator groove is hindered by Q738R substitution, but not by I603N and P671S substitutions.

Discussion

In this study we report 3 novel mutations in the *AR* gene, p.I603N, p.P671S, and p.Q738R, found in a cohort of 101 Indonesian DSD patients. All 3 patients presented with a PAIS phenotype. We performed extensive functional analyses of the mutant ARs to understand how these missense mutations correlate with the clinical phenotype of the patients. The results of our experiments are summarized in table 1.

Table 1. Summary of functional studies of androgen receptor mutants leading to partial androgen insensitivity syndrome

Mutant	Hyperphosphorylation (114-kDa isoform)	Transactivation	Coactivator binding	Transient immobilization
I603N	absent	−	+	−
P671S	present	±	+	+
Q738R	present	±	−	+

− = diminished, no activity; + = wildtype activity; ± = 50–75% wildtype activity.

The AR-I603N mutation is located in the DBD region of the AR, close to the D box in the 2nd zinc cluster. The D box is involved in AR dimerization and hormone-responsive element (HRE) half-site recognition. Amino acid substitutions in the D box normally result in a PAIS phenotype [Giwercman et al., 2004]. Our results show that the AR-I603N mutation leads to a defective hormone-induced hyperphosphorylation of the protein and absence of the 114-kDa phosphoprotein band probably due to a disturbed DNA binding. AR-I603N displays a normal translocation to the nucleus upon hormone stimulation but has completely lost its DNA-binding capacity as shown by live cell imaging, which explains its total lack of transcriptional activity from 2 distinct promoters. Previously, we have shown that disrupted DNA binding underlies a complete androgen insensitivity syndrome (CAIS) phenotype of a patient harboring an A573D mutation in the 1st zinc cluster [Brüggenwirth et al., 1998; Farla et al., 2005]. However, despite the presence of an inactivating AR-I603N mutation, the patient presented with a PAIS phenotype and partly suppressed AMH levels. Examination of the DNA sequence of exon 3 showed, besides the mutant, also a wildtype nucleotide at position 2170 in DNA from blood cells of the patient (fig. 6), indicative for somatic mosaicism. A similar occurrence of somatic mosaicism has previously been reported in a PAIS patient harboring a wildtype *AR* and an *AR* with a premature stop codon in the NTD [Holterhus et al., 1997]. Variable tissue distribution of wildtype and mutant *AR* alleles may also underlie the PAIS phenotype of the AR-I603N patient.

The AR-P671S mutation is located in helix 1 of the LBD and encoded by exon 4 of the *AR* gene. This proline is highly conserved among human steroid receptors, underscoring an important role for this amino acid. AR-P671S substitution results in a reduced transcription activity to 78% at physiological hormone concentrations, which could be partly overcome by increasing the level of androgen. The reason for this decreased activity is not yet understood, because in all other functional assays the AR-P671S mutation behaved like wildtype AR. Hiort and colleagues [1996] reported a different mutation of the same amino acid residue, P671H, in a PAIS patient, although its effect on AR function has not been tested. Our data indicate that suboptimal AR functioning due to the P671S mutation may be the underlying cause of the PAIS phenotype in this patient.

AR-Q738 is located in the hydrophobic coactivator groove in the surface of the AR-LBD (fig. 4) [Dubbink et al., 2004; He et al., 2004; Hur et al., 2004]. The coactivator groove is essential for both cofactor binding via LxxLL- and FxxLF-like motifs and interaction with the FxxLF motif in the NTD. We have shown that AR-Q738R substitution does not affect the AR isoform pattern, intranuclear distribution and mobility, and DNA binding, but results in a 2-fold decreased transcriptional activity at high hormone concentrations. The effect on transcription is even more pronounced at lower, more physiological hormone levels, yielding only 10% of wildtype activity. Most likely, the underlying reason for loss of activity is the strongly diminished interaction with the AR FxxLF motif. Our data are in line with previous results showing that abrogation of N/C interaction via the coactivator groove reduced transcriptional activity [He et al., 2000; Dubbink et al., 2004]. According to crystal structures, residue Q738 makes hydrophobic contacts with the N-terminal F (F+1) of the AR FxxLF motif (fig. 4b) [He et al., 2004; Hur et al., 2004]. Substitution of the polar but uncharged glutamine residue by a charged arginine residue is probably not allowed because of interference with hydrophobic interactions with F+1, thus destabilizing the FxxLF motif interaction. It is likely that binding of AR cofactors that largely depends on AR interaction via the coactivator groove in the LBD is also negatively influenced by the Q738R mutation [Dubbink et al., 2004, 2006; van de Wijngaart et al., 2006]. Altogether, these data underscore the essential physiological role of AR-Q738 in FxxLF motif binding, including binding to the NTD, i.e., N/C interaction.

Several other amino acid substitutions in residues located in the hydrophobic coactivator groove are PAIS-associated. The F725L and I737T mutations disrupt the N/C terminal interaction [Quigley et al., 2004]. The L712F was found several times in PAIS patients, and the Q733H mutation displayed a mosaic pattern [Hiort et al., 1998].

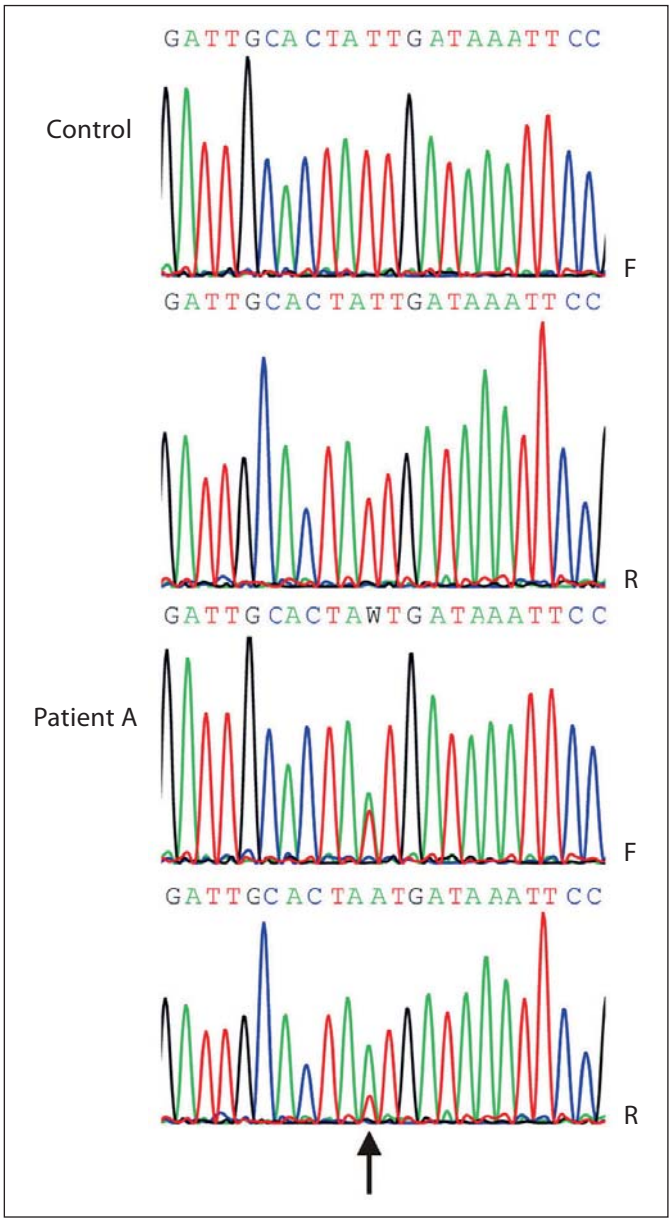

Fig. 6. Sequencing analysis pattern of a part of exon 3 of the *AR* gene in control DNA and DNA of patient A (Sequencing analysis version 5.3.1). The arrow indicates base pair position 2170 of the *AR* gene. F = Forward strand; R = reverse strand. In the basecalling panel W represents an A or T nucleic acid. In DNA from patient A a mosaic pattern is seen at position 2170.

In conclusion, we describe 3 novel PAIS-associated *AR* mutations present in the DBD (I603N), helix 1 of the LBD (P671S), and coactivator groove (Q738R) and provide insights in the clinical phenotypes of the patients harboring these mutations. AR-I603N entirely lost its DNA-binding capacity and transcriptional activity. Probably because of a somatic mosaicism, the patient displays a PAIS phenotype. The AR-P671S mutation interfered with transcriptional activity for as yet unclear reasons, and AR-Q738R replacement strongly reduced transcriptional activity because of abrogated capability to perform N/C interaction and cofactor binding. Altogether, our functional analysis of these mutants further increases the molecular understanding of AR functioning.

Acknowledgements

We thank Dr. Andrew Cato for supplying the pSG5AR expression plasmid, Dr. R. Dijkema for providing MMTV-Luc, Dr. G. Jenster for providing ARE_2-TATA-Luc, and Renske Olmer for excellent technical assistance.

References

Brüggenwirth HT, Boehmer AL, Lobaccaro JM, Chiche L, Sultan C, et al: Substitution of Ala564 in the first zinc cluster of the deoxyribonucleic acid (DNA)-binding domain of the androgen receptor by Asp, Asn, or Leu exerts differential effects on DNA binding. Endocrinology 139:103–110 (1998).

Claessens F, Verrijdt G, Schoenmakers E, Haelens A, Peeters B, et al: Selective DNA binding by the androgen receptor as a mechanism for hormone-specific gene regulation. J Steroid Biochem Mol Biol 76:23–30 (2001).

Dubbink HJ, Hersmus R, Verma CS, van der Korput HA, Berrevoets CA, et al: Distinct recognition modes of FXXLF and LXXLL motifs by the androgen receptor. Mol Endocrinol 18:2132–2150 (2004).

Dubbink HJ, Hersmus R, Pike AC, Molier M, Brinkmann AO, et al: Androgen receptor ligand-binding domain interaction and nuclear receptor specificity of FXXLF and LXXLL motifs as determined by L/F swapping. Mol Endocrinol 20:1742–1755 (2006).

Farla P, Hersmus R, Geverts B, Mari PO, Nigg AL, et al: The androgen receptor ligand-binding domain stabilizes DNA binding in living cells. J Struct Biol 147:50–61 (2004).

Farla P, Hersmus R, Trapman J, Houtsmuller AB: Antiandrogens prevent stable DNA-binding of the androgen receptor. J Cell Sci 118:4187–4198 (2005).

Giwercman YL, Ivarsson SA, Richthoff J, Lundin KB, Giwercman A: A novel mutation in the D-box of the androgen receptor gene (S597R) in two unrelated individuals is associated with both normal phenotype and severe PAIS. Horm Res 61:58–62 (2004).

Gottlieb B, Trifiro M, Lumbroso R, Vasiliou DM, Pinsky L: The androgen receptor gene mutations database. Nucleic Acids Res 24:151–154 (1996).

He B, Kemppainen JA, Wilson EM: FXXLF and WXXLF sequences mediate the NH2-terminal interaction with the ligand binding domain of the androgen receptor. J Biol Chem 275:22986–22994 (2000).

He B, Gampe RT Jr, Kole AJ, Hnat AT, Stanley TB, et al: Structural basis for androgen receptor interdomain and coactivator interactions suggests a transition in nuclear receptor activation function dominance. Mol Cell 16:425–438 (2004).

Hiort O, Sinnecker GH, Holterhus PM, Nitsche EM, Kruse K: The clinical and molecular spectrum of androgen insensitivity syndromes. Am J Med Genet 63:218–222 (1996).

Hiort O, Sinnecker GH, Holterhus PM, Nitsche EM, Kruse K: Inherited and de novo androgen receptor gene mutations: investigation of single-case families. J Pediatr 132:939–943 (1998).

Holterhus PM, Brüggenwirth HT, Hiort O, Kleinkauf-Houcken A, Kruse K, et al: Mosaicism due to a somatic mutation of the androgen receptor gene determines phenotype in androgen insensitivity syndrome. J Clin Endocrinol Metab 82:3584–3589 (1997).

Hughes IA: Disorders of sex development: a new definition and classification. Best Pract Res Clin Endocrinol Metab 22:119–134 (2008).

Hur E, Pfaff SJ, Payne ES, Gron H, Buehrer BM, Fletterick RJ: Recognition and accommodation at the androgen receptor coactivator binding interface. PLoS Biol 2:E274 (2004).

Jenster G, van der Korput HA, van Vroonhoven C, van der Kwast TH, Trapman J, Brinkmann AO: Domains of the human androgen receptor involved in steroid binding, transcriptional activation, and subcellular localization. Mol Endocrinol 5:1396–1404 (1991).

Jenster G, de Ruiter PE, van der Korput HA, Kuiper GG, Trapman J, Brinkmann AO: Changes in the abundance of androgen receptor isotypes: effects of ligand treatment, glutamine-stretch variation, and mutation of putative phosphorylation sites. Biochemistry 33:14064–14072 (1994).

Kuiper GG, de Ruiter PE, Trapman J, Jenster G, Brinkmann AO: In vitro translation of androgen receptor cRNA results in an activated androgen receptor protein. Biochem J 296:161–167 (1993).

Lubahn DB, Joseph DR, Sar M, Tan J, Higgs HN, et al: The human androgen receptor: complementary deoxyribonucleic acid cloning, sequence analysis and gene expression in prostate. Mol Endocrinol 2:1265–1275 (1988).

Quigley CA, De Bellis A, Marschke KB, el-Awady MK, Wilson EM, French FS: Androgen receptor defects: historical, clinical, and molecular perspectives. Endocr Rev 16:271–321 (1995).

Quigley CA, Tan JA, He B, Zhou ZX, Mebarki F, et al: Partial androgen insensitivity with phenotypic variation caused by androgen receptor mutations that disrupt activation function 2 and the NH(2)- and carboxyl-terminal interaction. Mech Ageing Dev 125:683–695 (2004).

Steketee K, Berrevoets CA, Dubbink HJ, Doesburg P, Hersmus R, et al: Amino acids 3–13 and amino acids in and flanking the 23FxxLF27 motif modulate the interaction between the N-terminal and ligand-binding domain of the androgen receptor. Eur J Biochem 269:5780–5791 (2002).

Trapman J, Dubbink HJ: The role of cofactors in sex steroid action. Best Pract Res Clin Endocrinol Metab 21:403–414 (2007).

van de Wijngaart DJ, van Royen ME, Hersmus R, Pike AC, Houtsmuller AB, et al: Novel FXXFF and FXXMF motifs in androgen receptor cofactors mediate high affinity and specific interactions with the ligand-binding domain. J Biol Chem 281:19407–19416 (2006).

van Royen ME, Cunha SM, Brink MC, Mattern KA, Nigg AL, et al: Compartmentalization of androgen receptor protein-protein interactions in living cells. J Cell Biol 177:63–72 (2007).

van Royen ME, Farla P, Mattern KA, Geverts B, Trapman J, Houtsmuller AB: Fluorescence recovery after photobleaching (FRAP) to study nuclear protein dynamics in living cells. Methods Mol Biol 464:363–385 (2009).